Electronic structure of heavily doped polyacetylene

Leif A. Eriksson
Department of Quantum Chemistry, Uppsala University, Box 518, S 751 20 Uppsala, Sweden

Michael Springborg
Fakultät für Chemie, Universität Konstanz, W 7750 Konstanz, Federal Republic of Germany
(Received 6 April 1992; revised manuscript received 31 July 1992)

We present results of first-principles, density-functional calculations on isolated *trans*-polyacetylene chains doped periodically at 100% and 33% concentration with Li, Be, B, C, N, O, F, Ne, or Na atoms as well as results for undoped chains. We focus on the electronic orbitals and have not attempted to optimize the structures. The results indicate the presence of non-negligible interactions between the orbitals of the dopants and those of the polymer, as seen, e.g., in a broadening of the energy ranges spanned by the dopant orbitals and in a fractional electron transfer between dopants and polymer. Although the calculations suffer from various approximations, these results—observed for all the dopants—allow us to make more general conclusions about the nature of polyacetylene when doped at lower concentrations and/or with other dopants. It is thus suggested that the experimentally observed doping-induced increase in electrical conductivity also is due to interchain interactions mediated through the dopants, in agreement with the experimental results of Bernier and co-workers. Finally, as a by-product our results demonstrate inaccuracies in electron transfers when studying weakly interacting systems using local-density calculations.

I. INTRODUCTION

About 15 years ago Chiang *et al.*[1] reported that the electrical conductivity of polyacetylene could be increased by many orders of magnitude upon doping. Similar properties have in the meanwhile been reported for a number of other related materials, and a large research activity in the properties of the conjugated polymers is currently been undertaken (see, e.g., Ref. 2).

Su, Schrieffer, and Heeger[3,4] offered an explanation for these observations according to which the dopants act as passive electron reservoirs which only donate or accept extra electrons to or from the polyacetylene chains. The charge can be carried along the single polymer chains with only little resistivity by means of solitons. According to this model the role of the dopants is limited and the effects of the finite size of the chains and of interchain interactions are ignored. Nevertheless, the model is believed to give the qualitatively correct description of the system, although details of the predictions of the model deviate from experimental findings (see, e.g., Refs. 5 and 6).

The role of the dopants may, however, be less secondary than originally assumed in the model of Su, Schrieffer, and Heeger. It is the purpose of the present paper to report results of a study exploring this question. We have performed first-principles calculations on an isolated, periodic, infinite chain of *trans*-polyacetylene doped at the very high levels of 100% or 33% with single Li, Be, B, C, N, O, F, Ne, or Na atoms. Our aim is to study the electronic orbitals, in particular those closest to the Fermi level since these are the ones determining the conducting properties of the polymer. We will focus on electronic energy bands and wave functions and have therefore not attempted to optimize structural parameters. It should be stressed that some of the dopants are unrealistic from a chemical perspective. However, performing the model study for the whole above-mentioned series of dopants allows general conclusions to be drawn that should be applicable also for more realistic materials (i.e., for other dopants and/or conjugated polymers, other concentrations, other geometries, and for dopants embedded in a multichain environment).

Before reporting the results of the present study we will put them into perspective compared with other studies on doped polyacetylene. It has been experimentally demonstrated that highly oriented polyacetylene samples possess a crystal structure in which the polymer axes are parallel. Doping these (e.g., with Li, K, Na, Cs, or Rb) may lead to slightly modified relative arrangements of the polyacetylene chains. Thereby channels between more chains are created inside which the dopants are placed (see, e.g., Refs. 7–14), and lead to situations in which the dopants are placed symmetrically between the chains.

Of the few available theoretical studies in which the modifications of the electronic properties of polyacetylene due to dopants are included, these mainly consider the dopants as solely giving rise to an extra electrostatic potential in which the π electrons of the polymer chains move (see, e.g., Refs. 15–19). In a series of papers,[20–22] Bernier and co-workers have, however, reported electron-spin-resonance (ESP) results that show that the spin of the charge carriers in the doped material couples to that of the nuclei of the dopants. This observation suggests that the dopants play a far more active role in the charge-transport processes.

To our knowledge there exist only a few other theoretical studies of the electronic properties of polyacetylene+dopant complexes. Most of these[23–29] as-

sume the Hartree-Fock approximation is a good approximation, which, however, may not be fully justified as the systems often are metallic. In contrast, our study and that of Kasowski, Caruthers, and Hsu[30] are based on the Hohenberg-Kohn density-functional formalism, which treats metals and semiconductors/insulators on the same footing.

Furthermore, almost all previous studies have each focused on one or two types of dopants (Li in Refs. 23, 25, 26, and 28, Na in Ref. 29, K and I in Ref. 24, H_2 and LiH in Ref. 27, but AsF_5, AsF_6, SbF_6, and PF_6 in Ref. 30), such that there have been no systematic studies as the one to be presented here.

The paper is organized as follows. In Sec. II we describe briefly the computational method as well as the structures we have considered. Section III contains the results, which are discussed further in Sec. IV. We conclude in Sec. V.

II. THEORETICAL METHOD

The computational method has been described in detail elsewhere[31–33] and we therefore only give a few basic principles here. Assuming the Born-Oppenheimer approximation to be valid, we make use of the Hohenberg-Kohn density-functional formalism.[34] The eigenfunctions to the Kohn-Sham equations[35]

$$\left[-\frac{\hbar^2}{2m}\nabla^2+V_N(\mathbf{r})+V_C(\mathbf{r})+V_{\rm xc}(\mathbf{r})\right]\psi_i(\mathbf{r})=\epsilon_i\psi_i(\mathbf{r}) \quad (1)$$

are expanded in a basis of linearized muffin-tin orbitals (LMTO's). A set consisting of two functions on each site and for each set of (l,m) is used, and s, p, and d functions are included on all sites. As discussed elsewhere, this basis set is constructed to produce good approximations to the exact solutions of Eq. (1), although of limited size. It should be stressed that we do not make any shape approximation for the potential.

Equation (1) is a single-particle equation, and the potential $V_C+V_{\rm xc}$ depends only on the total electron density

$$\rho(\mathbf{r})=\sum_i^{\rm occ}|\psi_i(\mathbf{r})|^2 . \quad (2)$$

V_N is the electrostatic potential of the nuclei and V_C is that of the electrons. For the exchange-correlation potential $V_{\rm xc}$ we use the local approximation of von Barth and Hedin.[36]

With our computer codes we can study the properties of quasi-one-dimensional materials, which are characterized as being isolated, periodic, helical, and infinite, and having a linear polymer axis. We make explicit use of the helical periodicity by constructing helical Bloch waves. We use a reduced k vector with $k=0$ and $k=1$ being the zone center and zone edge, respectively. A total of six k points in the interval from 0 to 1 was used in the present study. Since many of the systems are found to be metallic, this number may be considered too small for obtaining a detailed description of the materials. However, since we here focus on trends, the limited number of k points is acceptable. Finally, in the present study a special case of the helical periodicity is considered, namely the zigzag symmetry.

The 1s electrons of Li, Be, B, C, N, O, F, and Ne and the 1s and 2s electrons of Na are described within a frozen-core approximation. Moreover, although it may be relevant to allow the electrons to spin polarize, this degree of freedom was not considered.

We will focus on a few key quantities, including the single-particle band structures and the densities of states. In addition we will examine the Mulliken populations. For these we consider the atomic net populations of the dopants for the single orbitals as a function of the corresponding band energy. However, since more bands may appear in the same energy region and since we use a discrete set of k points we stress that the atomic net population as a function of the band energy does not appear as a smooth function. In the limit of a continuous k variable, the population as a function of the band energy will not appear as a single-valued function but rather as a more or less broadband. The discrete k mesh may instead lead to a rapidly oscillating function.

Furthermore, according to our definition of the net populations they also contain overlap populations between equivalent atoms from different unit cells (see Ref. 33). Besides studying the atomic net population of the dopants for the single orbitals, we also quote the calculated total atomic net populations (n_i) and the total atomic overlap populations ($n_{ij}, i\neq j$), as well as the total atomic gross populations (N_i).

The two structures shown in Fig. 1 were considered in the present work. By using the zigzag symmetry the

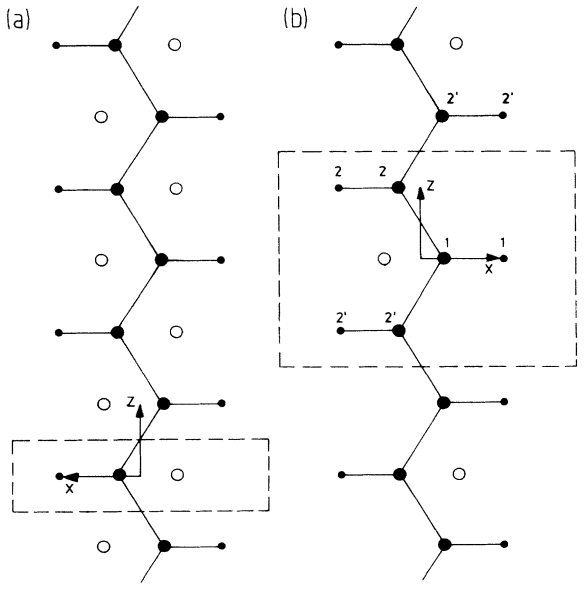

FIG. 1. Schematic representation of (a) 100% and (b) 33% doped *trans*-polyacetylene. The carbon and hydrogen atoms are represented by the larger and smaller filled circles, respectively, whereas the dopants are represented by the empty circles. The polyacetylene backbone is placed in the $y=0$ plane, and the dopants in the $|y|=3.5$ a.u. planes. For more details the reader is referred to the text.

100%-doped polyacetylene chain of Fig. 1(a) consists of unit cells of only three atoms, whereas that with 33% doping has seven atoms per unit cell. The "naked" polyacetylene chain was placed in the (x,z) plane. The C-C bond lengths were set equal to 2.65 a.u., and the effects of a bond-length alternation were accordingly neglected. The C-H bond lengths were set equal to 2.10 a.u., and all C-C-C and C-C-H bond angles were assumed to be 120°. This gives us carbon atoms at $(x,z)=(0.663,2n\times 2.295)$ a.u. and at $[-0.663,(2n+1)\times 2.295]$ a.u., where n is an integer. The dopants were placed at $(x,y,z)=(-1.163,-3.5,2n\times 2.295)$ a.u. and at $[1.163,3.5,(2n+1)\times 2.295]$ a.u. for 100% doping, whereas 2.295 is to be replaced by 6.885 for 33% doping.

Our structure results in the following interatomic distances between the dopants and the atoms of the polyacetylene chain [see Fig. 1(b)]. The distance to the carbon atom 1 is 3.95 a.u., those to carbon atoms 2 and 2′ are 4.22 a.u., that to hydrogen atom 1 is 5.26 a.u., and those to hydrogen atoms 2 and 2′ are 4.48 a.u. For 100% doping the shortest interatomic distances between the dopants are 4.59 and 7.73 a.u. The shorter distance especially is so small that we expect significant dopant-dopant interactions, such that the results may be obscured by them. For 33% doping the distances become 10.09 and 13.77 a.u. These are significantly larger than those for 100% doping, such that we expect the main dopant-dopant interactions to be absent for this structure.

Experiments for K- and Na-doped polyacetylene have revealed $|y|=4.5-6$ a.u.,[10,14,37] which is somewhat larger than our values. On the other hand, earlier theoretical studies have used distances between carbon and the dopants of around 4–5 a.u.,[23,25,26] and $|y|=2.8-4.1$ a.u.,[28,29] of which those of Refs. 25, 26, and 28 were optimized. Our chosen values thus appear appropriate.

The electron density plots will be shown in a plane with $y=1.75$ a.u. The x coordinate will range from -4 to $+4$ a.u., and the z coordinate from -6 to $+6$ a.u.

Finally, it should be stressed that we studied the effects of having different positions of the dopants by changing their $|y|$ values by ± 0.5 a.u. and their $|x|$ values by ± 0.25 a.u. The properties investigated in the present work were influenced very little by these structural modifications.

Before turning to our results we finally add two more points of relevance for the following discussion. Since the dopants are not placed in the plane of the polyacetylene chain, the symmetry is lowered and it is no longer possible to split the orbitals into σ and π orbitals. As a consequence, no two bands are allowed to cross in the band structures. A more fundamental aspect is that throughout the paper we will assume the eigenfunctions ψ_i and the corresponding eigenvalues ϵ_i [see Eqs. (1) and (2)] to be related to electronic orbitals and excitation values, respectively, although there is no strict justification for this. The experience from the past decades has, however, shown this to be a good approximation (see, e.g., Ref. 38).

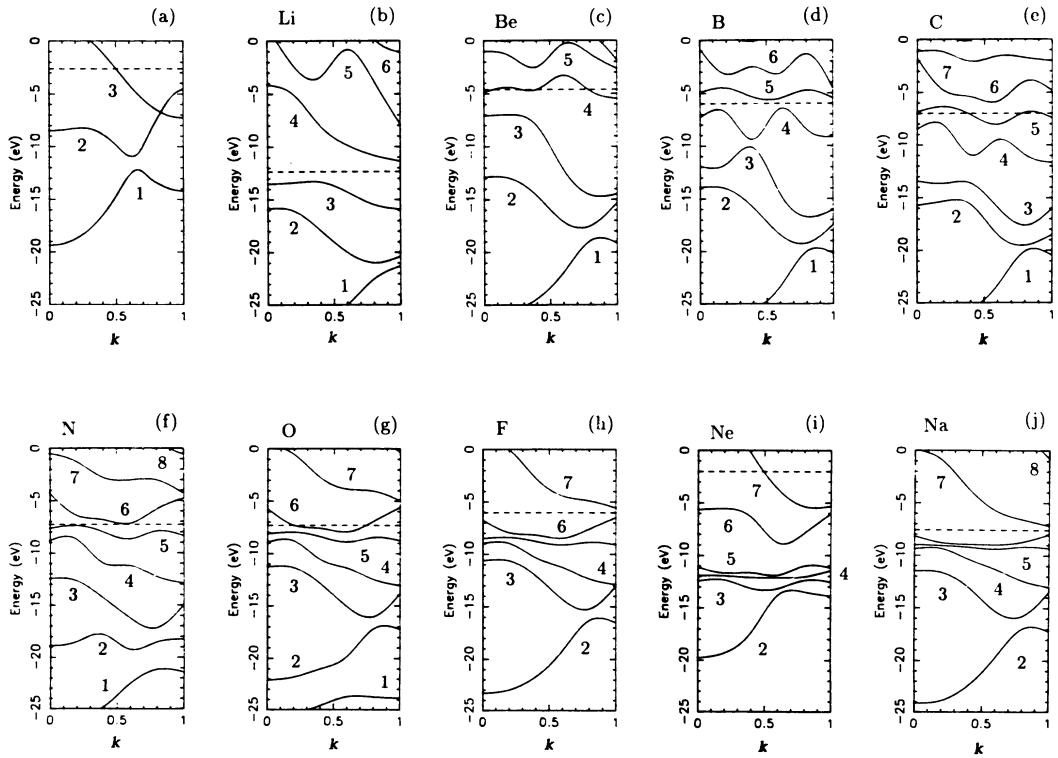

FIG. 2. Band structures of (a) pure undimerized *trans*-polyacetylene, and undimerized *trans*-polyacetylene doped 100% with (b) Li, (c) Be, (d) B, (e) C, (f) N, (g) O, (h) F, (i) Ne, and (j) Na. The dashed lines separate occupied and unoccupied orbitals. $k=0$ and $k=1$ are the zone center and zone edge, respectively. Only the bands between -25 and 0 eV are shown.

III. RESULTS

In Fig. 2 we show the band structures for the 100%-doped materials and in Fig. 3 for the materials with 33% dopants. In both figures we have included the band structures for the undoped *trans*-polyacetylene chains as calculated for the same structure as that used for the doped chains. The band structures of Fig. 2 are comparable with those presented in a preliminary report on the present work.[39]

When comparing the bands of Fig. 2 with those of Fig. 3, we immediately notice that the former are characterized by generally larger widths. Although this to some extent is due to the smaller unit cell, it also indicates that for the 100%-doped structures the dopants interact strongly. These dopant-dopant interactions are absent for lower (and thus more realistic) dopant concentrations. The results of Fig. 2 should therefore only be used in obtaining a qualitative insight into the properties of doped polyacetylene. On the other hand, a number of the bands in Fig. 3 are so narrow that the corresponding orbitals are fairly well localized in position space. These are localized mainly to the dopants, which thus to a large extent become almost noninteracting.

Figure 4 shows the densities of states corresponding to the band structures of Fig. 3, and Fig. 5 depicts the Mulliken atomic net populations on the dopants as functions of band energy. A comparison between Figs. 4 and 5 gives a direct picture of the positions of the dopant-derived orbitals. Figures 6–10 show, for some of the dopants and the bare polymer chain, the electron density of a few selected frontier orbitals in the plane described in Sec. II. In order to help the interpretation of the results in Figs. 6–10, Fig. 6(f) shows the underlying backbone of the polymer and the positions of the dopants. Finally, Tables I and II contain selected Mulliken populations and a few single-particle energies.

Except for Be, B, and Ne, all dopants lead to atomic gross populations on the dopants (N_X), which are larger than their number of valence electrons (Z_{eff}) (see Tables I and II). The exception of Ne is easily ascribed to the inertness of that element, and the difference $|N_X - Z_{\text{eff}}|$ can thus be taken as a rough estimate of the errors in interpreting N_X as the number of valence electrons on a particular dopant atom. The exception of B can be explained by comparable ionization potentials of the isolated B atoms and the isolated *trans*-polyacetylene chains. For Be one should expect a fairly small charge transfer due to the closeness of the Be 2*s* shell. That this is not found indicates that the Be 2*s* orbitals are so extended that there is a non-negligible interaction between the dopants and the polymer. This is supported by the fact that Be is that dopant for which N_X shows the largest difference between the 33% and the 100% doped materials, proposing significant interactions between the Be atoms in the 100% doped case. It is finally surprising that $N_X > Z_{\text{eff}}$ for Li and Na. A possible explanation of this is errors in the local-density approximation, as will be discussed in the next section.

The atomic net populations on the dopants as functions of band energy (Fig. 5) indicate the shell structure of the atoms. Passing through the series Be-Ne we recog-

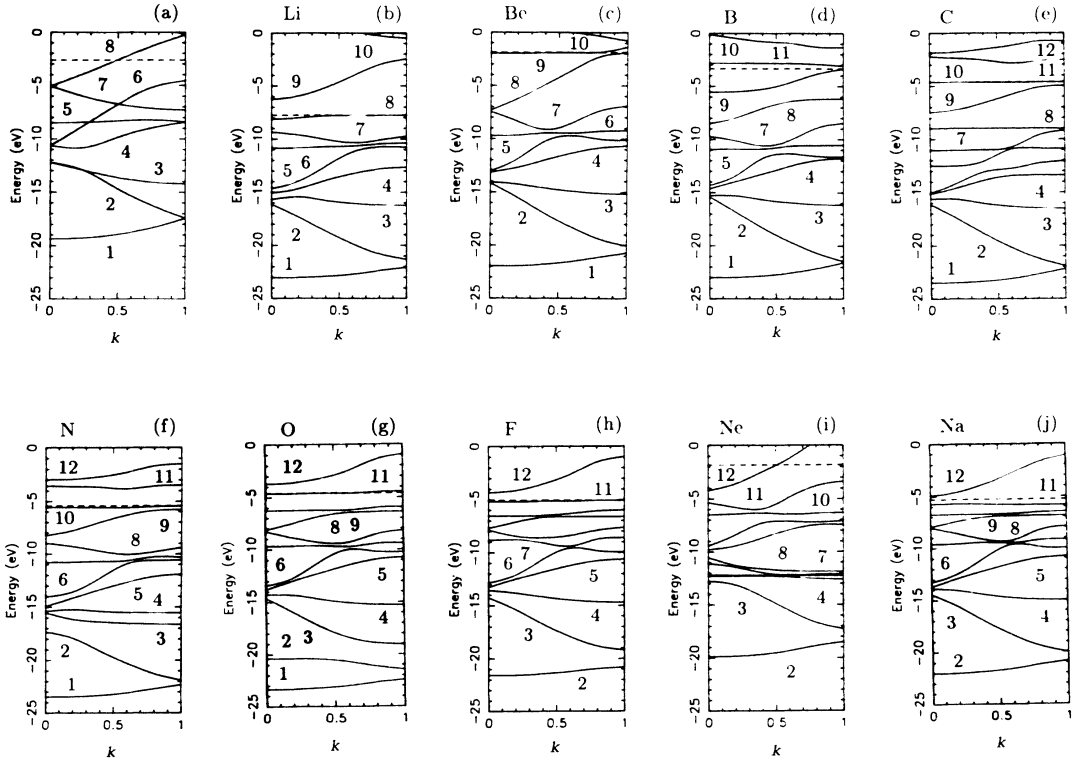

FIG. 3. As Fig. 2, except that the concentration of dopants in (b)–(j) is 33% and that the bands in (a) have been obtained from those of Fig. 2(a) by tripling the unit cell.

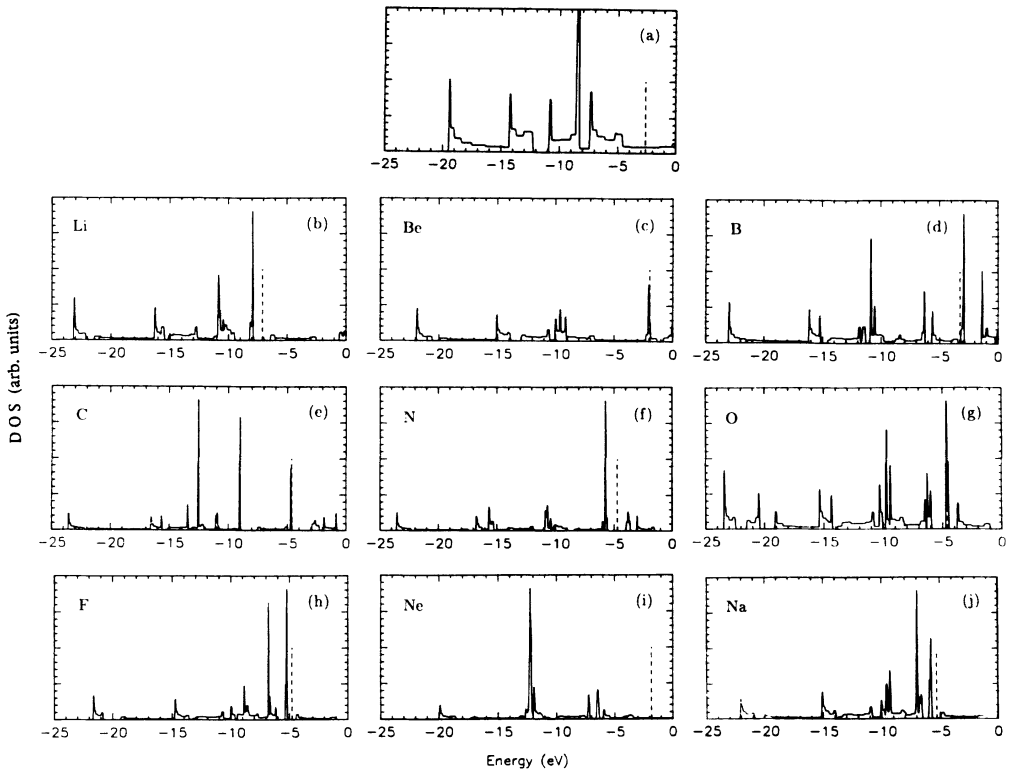

FIG. 4. The densities of states corresponding to the band structures of Fig. 3. The vertical dashed lines separate occupied and unoccupied orbitals. The curves do *not* have common ordinate scales.

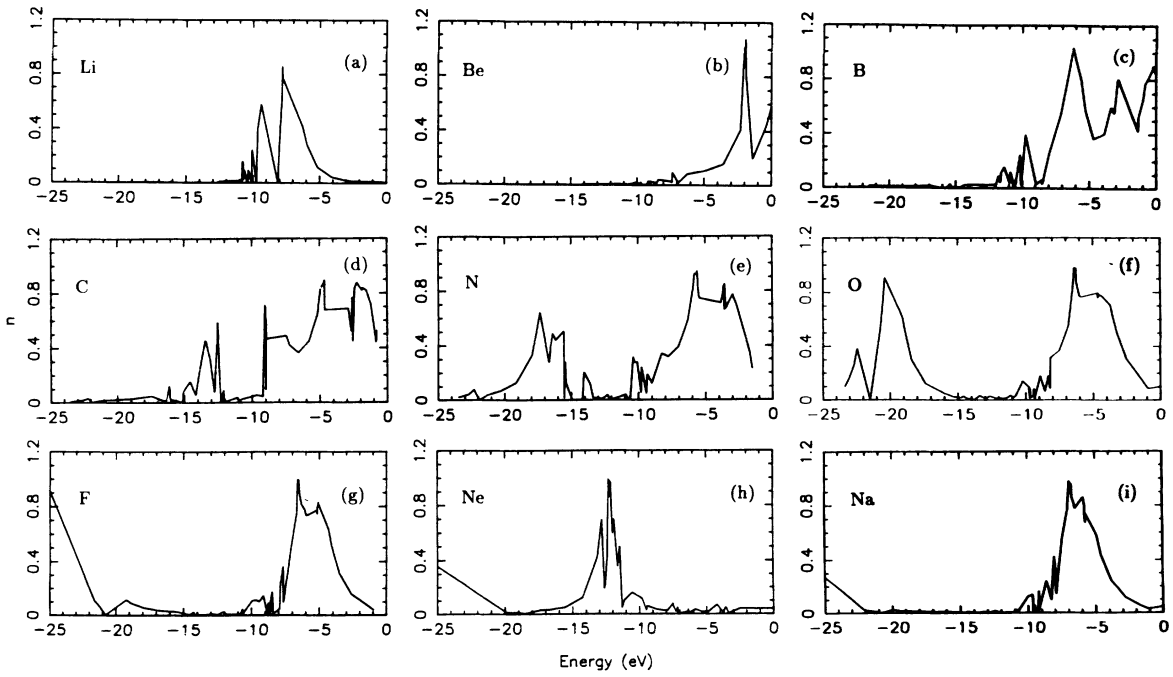

FIG. 5. The Mulliken net atomic population on the dopant as a function of band energy for *trans*-polyacetylene doped 33% with (a) Li, (b) Be, (c) B, (d) C, (e) N, (f) O, (g) F, (h) Ne, and (i) Na.

TABLE I. Various quantities as calculated for 100% doped polyacetylene. The dopants are labeled X and their effective nuclear charge (equal to their number of valence electrons) Z_{eff}. n_X, n_C, and n_H are the total Mulliken net population on the dopants, the carbon atoms, and the hydrogen atoms, respectively, whereas $n_{X,C}$ and $n_{X,H}$ are the overlap populations between the dopants and the carbon and hydrogen atoms, respectively. The Mulliken gross populations are labeled N_X, N_C, and N_H, respectively. For reference, the second column contains the results for the undoped material.

X		Li	Be	B	C	N	O	F	Ne	Na
Z_{eff}		1	2	3	4	5	6	7	8	7
n_X		1.59	1.88	2.98	4.09	5.23	6.22	7.23	8.03	7.30
n_C	3.58	3.04	3.51	3.54	3.46	3.44	3.35	3.29	3.45	3.08
n_H	0.85	0.73	0.86	0.84	0.83	0.83	0.83	0.83	0.93	0.79
$n_{X,C}$		0.07	0.04	−0.03	0.01	−0.07	0.04	0.09	0.00	0.19
$n_{X,H}$		0.01	0.05	0.03	−0.03	−0.06	−0.07	−0.06	−0.08	−0.01
N_X		1.63	1.92	2.99	4.08	5.17	6.20	7.24	7.98	7.39
N_C	3.87	3.36	3.86	3.85	3.78	3.72	3.69	3.65	3.79	3.50
N_H	1.13	1.01	1.22	1.17	1.14	1.11	1.11	1.11	1.23	1.11

nize two maxima (due to the $2s$ and $2p$ orbitals, respectively), which gradually move toward lower energy with increasing atomic number. The broadening of the "peaks" as observed in Fig. 5 is due to the interaction with the polyacetylene chain. With some good will this broadening is seen to decrease with increasing atomic number, which can be explained by the larger compactness of the atomic orbitals. In particular the Ne $2p$ peak is significantly narrower than the other dopant $2p$ peaks.

The difference between the atomic net populations and the atomic gross populations is solely due to the overlap populations, and a comparison between these for any atom therefore gives the total overlap population of the atom of interest. Such a comparison (cf. Table II) reveals that the overlap populations contribute with about 1.3, 0.3, and 0.1 to the atomic gross populations for the carbon atoms and the hydrogen atoms of the polymer backbone, and for the dopants, respectively. Hence, the interaction between the dopants and the polyacetylene backbone has only a smaller—although non-negligible—covalent component.

A comparison between the densities of states (Fig. 4) and the Mulliken net populations (Fig. 5) shows that the peaks in the latter correspond to peaks in the former. This is a further indication that the dopant-induced orbitals are largely atomiclike and accordingly give rise to bands with little dispersion. This is most pronounced for Ne, as should be expected. It should be added that further peaks in the densities of states can be related to the bands of the pure polyacetylene backbone, as demonstrated by a comparison between Fig. 4(a) and the other parts of Fig. 4. For lower dopant concentrations the densities of states are expected to resemble those of Fig. 4, although with a reduction in the height of the dopant-

TABLE II. Various quantities as calculated for 33% doped polyacetylene. The results are presented as in Table I with the extension that there are now two different types of carbon and hydrogen atoms labeled as in Fig. 1(b). Moreover, the positions (in eV) of the bottom of the band with dominating $(CH)_x$ components (ϵ_0) and of the Fermi level (ϵ_F) are included.

X		Li	Be	B	C	N	O	F	Ne	Na
Z_{eff}		1	2	3	4	5	6	7	8	7
n_X		1.81	1.78	3.01	4.21	5.34	6.46	7.51	8.09	7.56
n_{C_1}		2.31	2.57	2.54	2.47	2.42	2.38	2.40	2.53	2.38
n_{C_2}		2.41	2.55	2.52	2.48	2.45	2.42	2.44	2.51	2.42
n_{H_1}		0.83	0.90	0.88	0.86	0.86	0.86	0.87	0.92	0.86
n_{H_2}		0.82	0.89	0.87	0.85	0.85	0.87	0.86	0.92	0.85
n_{X,C_1}		0.11	0.08	0.13	0.16	0.15	0.13	0.13	0.06	0.10
n_{X,C_2}		−0.05	−0.04	−0.03	−0.01	0.01	−0.03	−0.07	−0.10	−0.01
n_{X,H_2}		−0.04	−0.04	−0.04	−0.05	−0.06	−0.09	−0.10	−0.09	−0.03
N_X		1.77	1.73	2.99	4.21	5.36	6.39	7.40	7.92	7.56
N_{C_1}	3.87	3.56	3.88	3.86	3.79	3.74	3.69	3.67	3.78	3.61
N_{C_2}	3.87	3.66	3.88	3.82	3.77	3.74	3.73	3.75	3.83	3.71
N_{H_1}	1.13	1.10	1.20	1.17	1.15	1.13	1.14	1.14	1.21	1.12
N_{H_2}	1.13	1.12	1.21	1.17	1.15	1.14	1.16	1.15	1.21	1.14
ϵ_0	−19.4	−23.1	−21.9	−23.0	−23.5	−23.5	−23.4	−21.6	−19.9	−22.0
ϵ_F	−2.6	−7.8	−2.0	−3.3	−4.6	−4.7	−4.6	−4.8	−1.8	−5.3

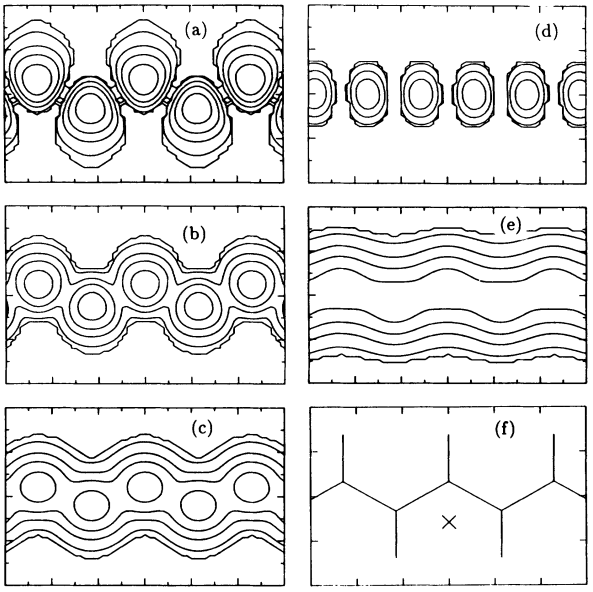

FIG. 6. Electron densities for some selected orbitals for undoped undimerized *trans*-polyacetylene in a plane parallel to that of the polymer backbone but 1.75 a.u. away from it. The contour values are 0.10, 0.08, 0.06, 0.04, 0.02, 0.01, 0.005, 0.002, and 0.001 a.u. The contour curves for the smaller value have a tendency to be the least smooth curves, which makes them recognizable. The size of the planes is 12×8 a.u. Referring to Fig. 2(a), the chosen orbitals are (a) band 3 for $k=\frac{1}{3}$, (b) band 3 for $k=\frac{1}{2}$, (c) band 3 for $k=\frac{2}{3}$, (d) band 2 for $k=1$, and (e) band 3 for $k=1$. The orbitals of (c), (d), and (e) are occupied, that of (a) is empty, and that of (b) is at the Fermi level. For reference, (f) shows the underlying polymer backbone as well as the position of the only dopant (X) in the region of the figure.

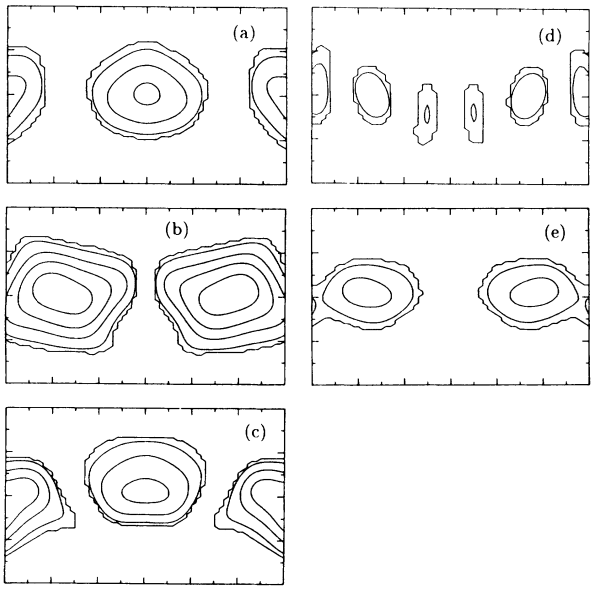

FIG. 7. Electron densities for selected orbitals for *trans*-polyacetylene doped 33% with Li as Fig. 6. The orbitals are [see Fig. 3(b)] (a) band 7 for $k=0$, (b) band 8 for $k=0$, (c) band 9 for $k=0$, (d) band 7 for $k=1$, and (e) band 8 for $k=1$. The orbitals of (a), (b), (d), and (e) are occupied, that of (c) is empty.

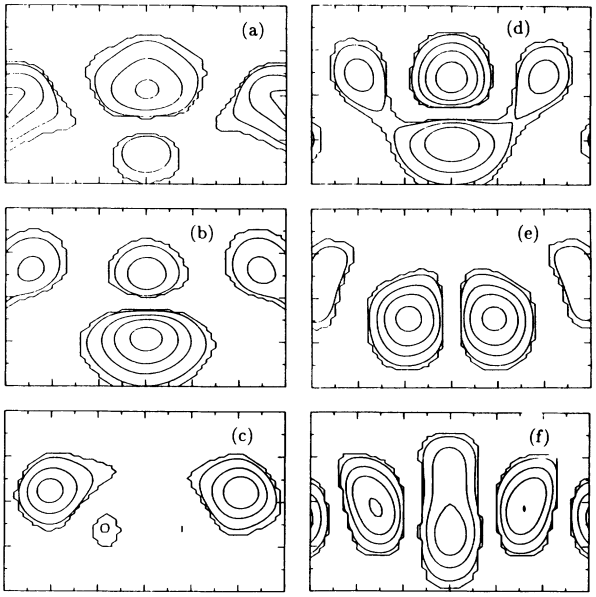

FIG. 8. Electron densities for selected orbitals for *trans*-polyacetylene doped 33% with B as Fig. 6. The orbitals are [see Fig. 3(d)] (a) band 9 for $k=0$, (b) band 10 for $k=0$, (c) band 11 for $k=0$, (d) band 9 for $k=1$, (e) band 10 for $k=1$, and (f) band 11 for $k=1$. The orbitals of (a) and (d) are occupied, those of (b), (c), (e), and (f) are empty.

induced peaks relative to those of the polymer backbone. This should be taken into account when comparing the results of Fig. 4 with those of experimental optical studies of doped conjugated polymers.

In Fig. 3 the occurrence of many bands in the neigh-

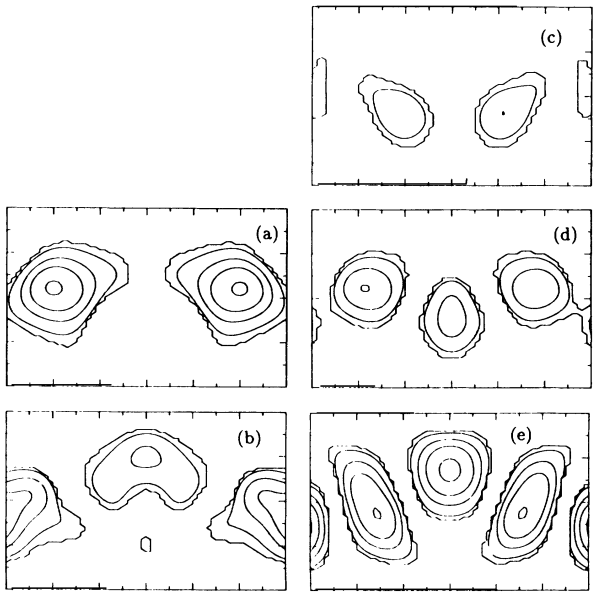

FIG. 9. Electron densities for selected orbitals for *trans*-polyacetylene doped 33% with F as Fig. 6. The orbitals are [see Fig. 3(h)] (a) band 11 for $k=0$, (b) band 12 for $k=0$, (c) band 10 for $k=1$, (d) band 11 for $k=1$, and (e) band 12 for $k=1$. The orbitals of (a), (c), and (d) are occupied, those of (b) and (e) are empty.

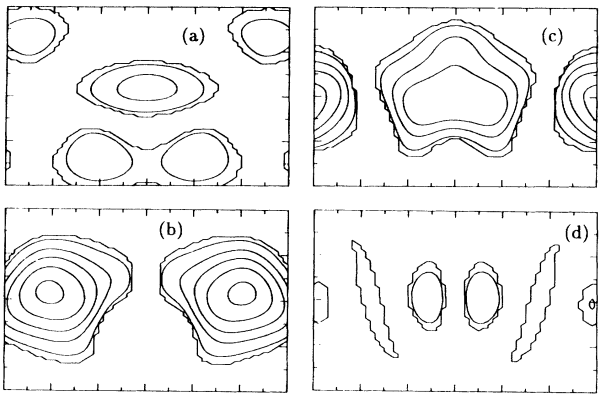

FIG. 10. Electron densities for selected orbitals for *trans*-polyacetylene doped 33% with Ne as Fig. 6. The orbitals are [see Fig. 3(i)] (a) band 10 for $k=0$, (b) band 11 for $k=0$, (c) band 12 for $k=0$, and (d) band 11 for $k=1$. All orbitals are occupied.

borhood of the Fermi level can be observed. Although many of these bands have large components on the dopants, they also have important contributions from the polyacetylene backbone (cf. Figs. 6–10).

The variation in ϵ_0 (Table II) is significantly smaller than that in ϵ_F. This is consistent with a picture in which the largest interactions between the dopants and the polymer are through the relatively delocalized π-derived orbitals of the polymer. A variation in the shape or occupation of these π orbitals will only slightly modify the single-particle energies of the localized σ bonds between the carbon atoms of the polymer. A further indication of this is the fact that the lowest two bands in Fig. 3(a) interact little with the orbitals of the dopants and are therefore recognizable for most of the 33% doped materials. On the other hand, these results indicate that a change in dimerization of the polymer backbone (including the occurrence of solitons and polarons) might be obtained as a result of these dopant-polymer interactions.

Finally, our total energy as a function of the positions of the dopants indicates—for the structural parameters we have considered—a net attraction between the dopants and the polymer for the dopants to the left in the Periodic Table and a net repulsion for those to the right. This is consistent with the trends in the total Mulliken overlap populations between the dopants and the polymer as reported in Table II.

IV. DISCUSSION

The most important findings of the preceding section are the following. There are significant orbital interactions between the dopants and the polymer which most clearly show up in the broad Mulliken net populations on the dopants as functions of band energy (Fig. 5). Furthermore, only fractions of an electron are transferred between the dopants and the polymer, and dopant-derived orbitals appear in most cases in the closest neighborhood of the Fermi level. A rigid-band model in which the dopants solely donate or remove an integral number of electrons from the π bands of the polymer accordingly does not seem to be completely justified.

In the present section we will address the question of how the obtained results depend on the approximations made in the calculations; i.e., on the lack of spin polarization, on the local-density approximation, on the lack of bond-length alternation in the polymer backbone, and on the lack of multichain effects. Finally, we address the question of whether the results can be considered general for doped conjugated polymers.

Kasowski, Caruthers, and Hsu[30] presented density-functional results for crystalline polyacetylene heavily doped with AsF_5, AsF_6, SbF_6, and PF_6, together with results for the undoped material. Their results show strong modifications in the uppermost valence bands upon doping. Moreover, the dopant-derived levels appear in the nearest vicinity of the Fermi level and are those defining (major parts of the) frontier orbitals, except for the PF_6-doped material for which the band with dominating dopant components occurs about 2 eV above the Fermi level.[30]

In their *ab initio* Hartree-Fock study, Brédas, Chance, and Silbey[23] examined polyacetylene doped 33% with Li. In the region spanned by the filled valence π and the empty conduction π bands of the undoped material they observe two extra bands with major components on the Li atoms. In particular, one of those is found to be very flat. Of further relevance for the present study is their finding of only a fractional charge transfer between polyacetylene and Li.

Further theoretical studies[24,26,28] have also yielded a fractional electron transfer for doped polyacetylene. Other studies[25,27,40] support our findings that there are dopant-induced levels close to the Fermi level. Our results thus are seen to agree with those of other theoretical studies on doped polyacetylene.

However, there is a discrepancy between our calculated electron transfer versus those derived from *ab initio* Hartree-Fock calculations on the Li- and Na-doped system and those expected from chemical intuition. Errors in the local-density approximations as well as the neglected spin polarization may be explanations for this, but the inability of the Hartree-Fock method to describe metallic systems also may be responsible for the difference. We shall return to the first proposal in more detail.

Since the dopant-polymer interactions are fairly small (compared with the covalent interactions inside the polymer) it is reasonable to compare our results with those of the system of noninteracting dopants and polymers; i.e., the isolated polyacetylene chain and the isolated dopant atoms. For the isolated polyacetylene chain we have previously demonstrated[41,33] that the method applied here does give results in good agreement with experiments.

On the contrary, Trickey[42] has calculated the ionization potentials of a number of isolated atoms within a spin-polarized local-density approximation and compared them with the experimental values. He found the theoretical values to lie consistently below the experimental values with a difference being about 2 eV for Li and Na, 4 eV for Be and B, 5 eV for C, 6 eV for O, 7 eV for F, and 8 eV for N and Ne. Thus, using a spin-polarized

local-density approximation the uppermost atomic levels will be too high in energy, with the largest discrepancy for the elements to the right in the Periodic Table. Assuming the bands for the bare polyacetylene chain to be shifted rigidly upwards (compared to the correct positions) by an amount that is dominated by the error for the isolated carbon atom (i.e., about 5 eV), the relative positions of the Li- or Na-induced bands will as a consequence be too low, whereas those of the F- and N-induced bands will be too high. This will result in too large a transfer of electrons from the polymer to the dopants for Li and Na and too small a transfer for F and N. Consequently, we estimate N_X to decrease for Li and Na and to increase for F and N, which will bring our results on the alkali-doped materials into better agreement with those of other studies. For the other dopants one also has to modify the electron transfers, but to a smaller extent.

As demonstrated by Jones and Gunnarsson,[38] the main differences between spin-polarized and spin-unpolarized local-density calculations for the atoms of our interest show up for the atoms to the right in the Periodic Table. The difference shows the same trend as that mentioned above (although smaller), strengthening the conclusions made.

For the 33% doped systems the dopant-dopant interatomic distances are so large that the corresponding interactions can be neglected. Thus, the observed broadening of the dopant levels (see, e.g., the Mulliken populations in Fig. 5) is due to orbital interactions between the dopants and the polymer and are accordingly expected also to be found for other (e.g., lower and hence more realistic) concentrations as well as for other distributions of the dopants (e.g., random or clustering). Moreover, these will also be fairly independent of the precise structure of polyacetylene chain. We notice that the occurrence of a broadening is general and also found for the inert-gas Ne. We will therefore expect it to be found for *any* dopant, whether atomic or molecular.

Due to the orbital interactions it is possible to have a fractional electron transfer between the dopants and the polymer. The size of this transfer is determined such that the Fermi levels of the two subsystems line up, and are thus sensible to the type and concentrations of the dopants as well as the structure and the number of the neighboring polymer chains. Regarding dopants for which the occupied and unoccupied orbitals are separated by not too large an energy gap, and for which the valence orbitals do not lie too deep in energy (as for most of the dopants considered here except for Ne), fractions of electrons may be transferred between the dopants and the polymer and enter or leave the band orbitals of the polymer. The occurrence of these extra charges on the polymer may lead to the formation of solitonic defects as originally proposed by Su, Schrieffer, and Heeger[3] for an integral electron transfer. The solitons may in turn be responsible for the large electrical intrachain conductivity and together with a dopant-assisted interchain hopping (through the orbital interactions) this gives a large macroscopic electrical conductivity for the doped materials. Furthermore, the presence of the dopants may modify the material from being quasi-one-dimensional to being more three dimensional through the orbital interactions such that the localization of the electrons due to the disorder is reduced, which also will lead to an increase in the electrical conductivity.

Due to this fractional electron transfer one has to be careful when discussing the variations in the physical properties of the doped materials as functions of dopant concentrations (see, e.g., Refs. 18 and 19), as the charge of the chains may be related to the dopant concentrations in a nonsimple fashion.

The interactions of the frontier orbitals are between dopant orbitals and π orbitals of the polymer. Since π orbitals are found to be the frontier orbitals for most conjugated polymers, we expect results similar to those presented here also to be found for other doped polymers. The actual size of the dopant-polymer electron transfer may be modified when considering dopants in a multichain environment. Some very simple model studies using a model Hamiltonian suggest, however, that the qualitative picture will remain unaltered when reducing the dopant concentration and when including multichain effects.

A very rough estimate of the size of the dopant-polymer hopping integrals may be obtained in the following way. We consider a periodic polymer chain with N_P Wannier orbitals per unit cell. The jth orbital of the nth unit cell is denoted ϕ_n^j. With on-site energies and nearest-neighbor hopping integrals equal to ϵ_P^j and t_P^j, respectively, the electronic Hamiltonian of the polymer becomes

$$\hat{H}_P=\sum_{j=1}^{N_P}\left[\epsilon_P^j\sum_n c_{j,n}^\dagger c_{j,n}+t_P^j\sum_n (c_{j,n+1}^\dagger c_{j,n}+c_{j,n}^\dagger c_{j,n+1})\right] . \tag{3}$$

We have here neglected the spin degree of freedom and let $c_{j,n}^\dagger$ and $c_{j,n}$ be the creation and annihilation operators for the jth Wannier orbitals of the nth unit cell.

The eigenvalues and eigenfunctions to the Schrödinger equation

$$\hat{H}_P\phi=\epsilon\phi \tag{4}$$

are the well-known

$$\epsilon=\epsilon_k^j=\epsilon_P^j+2t_P^j\cos(\pi k) \tag{5}$$

and

$$\phi=\phi^j(k)=\frac{1}{N^{1/2}}\sum_n e^{ikn\pi}\phi_n^j , \tag{6}$$

with

$$k\in[-1;1] \tag{7}$$

and N being the number of unit cells.

We now introduce a single dopant close to unit cell number 0 such that the lth dopant orbital $\phi_X^l(l=1,2,\ldots,N_X)$ will interact with the Wannier functions of unit cells -1, 0, and $+1$. The corresponding hopping integrals will be denoted t_{-1}^{jl}, t_0^{jl}, and t_{+1}^{jl}, respectively. We assume $t_{-1}^{jl}=t_{+1}^{jl}$.

The electronic Hamiltonian for the isolated dopant is

$$\hat{H}_X = \sum_{l=1}^{N_X} \epsilon_X^l c_{l,X}^\dagger c_{l,X} \ , \tag{8}$$

and the solutions to the corresponding Schrödinger equation become

$$\epsilon = e_X^l \tag{9}$$

and

$$\phi = \phi_X^l \ , \tag{10}$$

respectively.

The interaction between the dopant and the polymer is described by the electronic Hamiltonian

$$\hat{H}_{\rm int} = \sum_{j=1}^{N_P} \sum_{l=1}^{N_X} [t_0^{jl}(c_{j,0}^\dagger c_{l,X} + c_{l,X}^\dagger c_{j,0}) + t_1^{jl}(c_{j,-1}^\dagger c_{l,X} + c_{l,X}^\dagger c_{j,-1} + c_{j,+1}^\dagger c_{l,X} + c_X^\dagger c_{j,+1})] \ . \tag{11}$$

We focus on the changes in the dopant orbitals and seek accordingly for a particular dopant orbital ϕ_X^l the dominating dopant-polymer interactions (i.e., that j with the largest values of t^{jl}). For resonance

$$\epsilon_X^l = \epsilon_k^j \tag{12}$$

the eigenvalues become

$$\epsilon = \epsilon_X^l \pm [t_0^{jl} + 2t_1^{jl}\cos(k\pi)] \ . \tag{13}$$

Since t_0 and $t_{\pm 1}$ may be of comparable size [cf. Fig. 1(b)], Eq. (13) indicates a broadening of the Mulliken net populations of the order of roughly $4t_0$. From Fig. 5 we thus estimate $t_0 \simeq t_1 \simeq 0.5$ eV.

We stress finally that this value should only be considered as an order-of-magnitude estimate, due to the number of approximations applied in arriving at it.

V. CONCLUSIONS

In this model study we have performed first-principles density-functional calculations on a single periodic chain of *trans*-polyacetylene doped with various atoms ranging from Li to Na. For the low dopant concentration (33%, which is still large) the dopant-dopant interactions were found to be almost negligible, and the results could thus also provide some information about the materials with much lower dopant concentrations.

The shell structure of the atomic dopants could be recognized in the band structures, densities of states, electron densities, and Mulliken populations, although small but non-negligible interactions between the orbitals of the polymer and those of the dopants led to a broadening of the atomic levels. Despite the fact that some of the studied systems may not be experimentally realizable, the general trends in our results suggest that similar effects should be expected for other dopants, other concentrations, other dopant-polymer arrangements, and other conjugated polymers.

As a consequence of the orbital interactions the dopant-polymer interaction has a small covalent component, such that the electron transfer between the two subsystems need not be integral. Although inaccuracies in the local-density approximation excluded us from making accurate statements about the size of the electron transfer, we believe such fractional electron transfer to be a general phenomenon for doped conjugated polymers, except when the dopants are closed-shell systems with a large energy gap between occupied and unoccupied orbitals.

For almost all systems considered both dopant orbitals and polymer orbitals were found in the closest vicinity of the Fermi level. This, together with the above-mentioned orbital interactions, indicates that the large electrical conductivity in doped conjugated polymers is partly due to structural intrachain defects (e.g., solitons and polarons) and partly due to dopant-assisted hopping between the chains. This is in accordance with the experimental ESR results of Bernier and co-workers,[20–22] that the dopants are active in the charge transport processes.

Due to the fractional electron transfer one has to be careful in analyzing experimental data on physical properties of doped conjugated polymers as functions of dopant concentrations. Finally, a rough estimate predicted the dopant-polymer hopping integrals to be of the order of 0.5 eV.

For the system where an alkali metal (Li or Na) has been used as dopant, an erroneous direction of electron transfer is observed, compared with other theoretical studies. This unsatisfying discrepancy is explained as a consequence of the too low atomic ionization potentials obtained within the local- (spin-) density approximation.[42] As a by-product of our study it is therefore seen that one has to be careful when analyzing electron transfers in weakly interacting systems such as when using those obtained with local-density calculations.

ACKNOWLEDGMENT

This work was supported in part by the Swedish National Board for Technical Development within the framework of the ESPRIT Basic Research Action 3314.

[1] C. K. Chiang, C. R. Fincher, Jr., Y. W. Park, A. J. Heeger, H. Shirakawa, E. J. Louis, S. C. Gau, and A. G. MacDiarmid, Phys. Rev. Lett. **39**, 1098 (1977).

[2] *Proceedings of the International Conference on Science and Technology of Synthetic Metals, 1990, Tübingen* [Synth. Met. **41-43** (1991)].

[3] W. P. Su, J. R. Schrieffer, and A. J. Heeger, Phys. Rev. Lett. **42**, 1698 (1979).

[4] W. P. Su, J. R. Schrieffer, and A. J. Heeger, Phys. Rev. B **22**, 2099 (1980); **28**, 1138(E) (1983).

[5] A. J. Heeger, S. Kivelson, J. R. Schrieffer, and W.-P. Su, Rev. Mod. Phys. **60**, 781 (1988).

[6] D. Baeriswyl, D. K. Campbell, and S. Mazumdar, in *Conducting Polymers*, edited by H. Kiess (Springer, Heidelberg, 1991).

[7] W. Winokur, Y. B. Moon, A. J. Heeger, J. Barker, D. C. Bott, and H. Shirakawa, Phys. Rev. Lett. **58**, 2329 (1987).

[8]N. S. Murthy, L. W. Shacklette, and R. H. Baughman, J. Chem. Phys. **87**, 2346 (1987).
[9]N. S. Murthy, L. W. Shacklette, and R. H. Baughman, Phys. Rev. B **40**, 12 550 (1989).
[10]N. S. Murthy, L. W. Shacklette, and R. H. Baughman, Phys. Rev. B **41**, 3708 (1990).
[11]P. A. Heiney, J. E. Fischer, D. Djurado, J. Ma, D. Chen, M. J. Winokur, N. Coustel, P. Bernier, and F. E. Karasz, Phys. Rev. B **44**, 2507 (1991).
[12]N. Coustel, P. Bernier, and J. E. Fischer, Phys. Rev. B **43**, 3147 (1991).
[13]J. E. Fischer, P. A. Heiney, and J. Ma, Synth. Met. **41-43**, 33 (1991).
[14]F. Saldi, M. Lelaurian, and D. Billaud, Solid State Commun. **76**, 595 (1990).
[15]E. M. Conwell, H. A. Mizes, and S. Jeyadev, Phys. Rev. B **40**, 1630 (1989).
[16]E. M. Conwell, H. A. Mizes, and S. Jeyadev, Phys. Rev. B **41**, 5067 (1990).
[17]R. J. Cohen and A. J. Glick, Phys. Rev. B **42**, 7659 (1990).
[18]S. Stafström, Phys. Rev. B **43**, 9158 (1991).
[19]H. A. Mizes and E. M. Conwell, Phys. Rev. B **43**, 9053 (1991).
[20]F. Rachdi and P. Bernier, Phys. Rev. B **33**, 7817 (1986).
[21]A. El-Khodary and P. Bernier, J. Chem. Phys. **85**, 2243 (1986).
[22]C. Fite, A. El Khodary, and P. Bernier, Solid State Commun. **62**, 599 (1987).
[23]J. L. Brédas, R. R. Chance, and R. Silbey, J. Phys. Chem. **85**, 756 (1981).
[24]M. Kertesz, Int. J. Quantum Chem. **29**, 1165 (1986).
[25]C. Tanaka, J. Tanaka, and K. Hirao, Synth. Met. **17**, 19 (1987).
[26]L. A. Burke and K. Krogh-Jespersen, Int. J. Quantum Chem. Symp. **22**, 51 (1988).
[27]Y. Aoki, A. Imamura, and K. Morokuma, Theor. Chim. Acta (Berlin) **75**, 247 (1989).
[28]C. Yang, W. You-Liang, and C. Bo, Int. J. Quantum Chem. **37**, 679 (1990).
[29]C. Fredriksson and S. Stafström, Synth. Met. **44**, 65 (1991).
[30]R. V. Kasowski, E. Caruthers, and W. Y. Hsu, Phys. Rev. Lett. **44**, 676 (1980).
[31]M. Springborg and O. K. Andersen, J. Chem. Phys. **87**, 7125 (1987).
[32]M. Springborg, J. Chim. Phys. **86**, 715 (1989).
[33]M. Springborg, J.-L. Calais, O. Goscinski, and L. A. Eriksson, Phys. Rev. B **44**, 12 713 (1991).
[34]P. Hohenberg and W. Kohn, Phys. Rev. **136**, B864 (1964).
[35]W. Kohn and L. J. Sham, Phys. Rev. **140**, A1133 (1965).
[36]U. von Barth and L. Hedin, J. Phys. C **5**, 1629 (1972).
[37]N. S. Murthy, L. W. Shacklette, and R. H. Baughman, Bull. Am. Phys. Soc. **31**, 232 (1986).
[38]R. O. Jones and O. Gunnarsson, Rev. Mod. Phys. **61**, 689 (1989).
[39]M. Springborg, J.-L. Calais, O. Goscinski, and L. A. Eriksson, Synth. Met. **41-43**, 3309 (1991).
[40]J. L. Brédas, B. Thémans, J. G. Fripiat, J. M. André, and R. R. Chance, Phys. Rev. B **29**, 6761 (1984).
[41]M. Springborg, Phys. Rev. B **33**, 8475 (1986).
[42]S. B. Trickey, Phys. Rev. Lett. **56**, 881 (1986).